https://dx.doi.org/10.4314/dujopas.v10i4c.9
ISSN (Print): 2476-8316
ISSN (Online): 2635-3490
Dutse Journal of Pure and Applied Sciences (DUJOPAS), *Vol. 10 No. 4c December 2024*

Major Oxides Distribution, Provenance, and Tectonic Settings of the Mudstones from Gombe Formation, Gongola Basin, Upper Benue Trough, Nigeria

Abiodun B. Ogbesejana[1*], Sunusi Saleh[2,3], Adebayo Matthew Adeleye[4], Oluwasesan M. Bello[3], Augustine C. Egwu[5], Babangida M. Sarki Yandoka[6], Abdullahi Musa[3]

[1]Department of Industrial Chemistry,
Faculty of Physical Sciences,
Federal University Dutsin-Ma,
P.M.B. 5001,
Katsina State,
Nigeria.

[2]Department of Science Laboratory Technology,
Faculty of Science,
Hafed Polytechnic Kazaure,
P.M.B., 5363,
Kazaure, Jigawa State,
Nigeria.

[3]Department of Chemistry,
Faculty of Physical Sciences,
Federal University Dutsin-Ma,
P.M.B. 5001,
Katsina State,
Nigeria.

[4]Department of Chemistry,
University of Ibadan,
Oyo State,
Nigeria.

[5]BGI Laboratory Limited,
278 Port-Harcourt/Aba Expressway,
Port-Harcourt,
Rivers State,
Nigeria.

[6]Department of Geology,
Bayero University,
P.M.B. 3011,
Kano State,
Nigeria.

Email: abiodunogbesejana@gmail.com

Author for Correspondence

Abstract

The Gombe Formation in northeastern Nigeria contains mudstones, along with other sedimentary rocks like sandstones, shales, and coals. To date, however, the major oxides geochemical studies of these mudstones are still poorly documented. The present study investigated the geochemical importance of major oxides in the mudstones from Gombe formation, Upper Benue Trough, Nigeria by x-ray fluorescence spectrometry (XRF) within the context of provenance, tectonic environments, and paleosalinity. Among the twenty (20) major oxides identified, the mudstones exhibit elevated levels of SiO_2, with Al_2O_3 >Fe_2O_3>MgO>TiO_2>K_2O>BAO>SrO; whereas the remaining oxides demonstrated low concentrations. This suggests that mudstones were predominantly constituted of quartz minerals and were formed in marine settings. The relatively elevated levels of Fe_2O_3 (with an average of 3.36 %) and MgO (with an average of 2.48 %) in the samples indicated that the source rocks were likely to be mafic to ultramafic. The major oxides ratios in the mudstones indicated that the sediments were derived from a mixture of felsic igneous and mafic igneous rocks with mixed compositional maturity in close proximity to the active continental margin. This study showed that major oxides were effective in evaluating the provenance and tectonic settings of the mudstones from Gombe formation in Gongola Basin, Nigeria.

Keywords: Major oxides; provenance; tectonic settings; Gombe formation; x-ray fluorescence spectrometry.

INTRODUCTION

The Benue Trough (BT) in Nigeria represents a linear lithospheric zone that originated at the onset of the Cretaceous period through the separation of the West-Central African basement. This trough encompasses approximately 6000 meters of Cretaceous sediments, with those dating prior to the mid-Santonian exhibiting faulting, folding resultant from compressional forces, and uplift in various locations (Fatoye and Gideon, 2013b). Early investigations suggest that the formation of the trough resulted from the deposition of sediments by lacustrine and fluvial systems. Furthermore, Benkhelil (1989) asserts that the BT was established in the early Cretaceous epoch concomitant with the expansion of the Atlantic Ocean. From a geographical perspective, the BT extends in a NNE–SSW orientation, spanning a distance of 800 kilometers and a breadth of 150 kilometers (Petters, 1982). Obaje *et al.* (1999) have indicated that the southern boundary of the BT is situated at the northern limit of the Niger Delta, while its northernmost boundary is positioned to the south along the border with the Chad Basin (Fig. 1). It has been reported that the BT underwent tectonic evolutions significantly influenced by a system of axial faults characterized by strike-slip dynamics, localized compressive events, and tensile regimes (Benkhelil, 1989). The ensuing thermal disturbances, lithospheric stressors, and rheological conditions resulted in the formation of basement horsts and basins that either facilitated or constrained certain fault-related deformations (Benkhelil, 1989). Olade (1975) proposed a discernible model focused on the escalation and cessation of mantle upwelling beneath the Cretaceous hot spot. The corresponding manifestations of doming, magmatism, rifting, tectonism, and sedimentation are postulated for the rift zone within the BT. The BT is divided into three distinct segments, namely; the Lower, Middle, and Upper regions (Fig. 1). Although the demarcation of the various regions is not explicitly defined, the most significant towns (localities or villages) that serve as focal points for the different regions are extensively documented in the academic literature (Petters, 1982; Nwajide, 1990; Idowu and Ekweozor, 1993).

The Upper Benue Trough is known for its complex sedimentary sequences and rich mineral resources (Nwajide, 2013). It experienced a compressional phase at the end of Santonian and Maastrichtian which resulted in the folding and faulting of the sediments. It is divided into the N-S trending Gongola Basin and the E-W trending Yola Basin (Fig. 1) (Abubakar, 2014).

The Cretaceous sediments of the Gongola Basin are mainly composed of five sedimentary formations namely Bima, Yolde, Pindiga, Gombe and Kerri-kerri Formations. The Yola Basin is made up of Bima, Yolde, Dukul, Jessu, Sekuliye, Numanha and Lamja Formations (Fig. 2).

The Gombe Formation represents the most recent Cretaceous lithostratigraphic unit within the north-south oriented Gongola sub-basin of the Northern Benue Trough (Popoff et al., 1986; Nwajide, 2013). This formation is characterized by an unconformable relationship with the underlying Fika Shale and is succeeded by the overlying Palaeocene Keri-Keri Formation. The lithological components of the Gombe Formation are systematically classified into three distinct units (Zaborski *et al.*, 1997): the basal interbedded unit, the middle bedded facies, and the upper red sandstone facies. The basal unit is composed of alternating thin layers of silty shales, which incorporate plant detritus and fine to medium-grained sandstones interspersed with flaggy ironstones. The middle section is characterized by consistently horizontally bedded fine to medium-grained quartz arenite, interstratified with silts, silty clays, and ironstones; conversely, the upper segment of the formation is predominantly composed of brick-red sandstone. The grain sizes within the formation exhibit a range from pebble-sized to medium-grained sandstones, showcasing trough, tabular, and planar cross-bedding structures. The Gombe Formation is classified as Maastrichtian in age (Carter *et al*. 1963; Kogbe 1976; Popoff *et al.* 1986). Mudstone, a sedimentary rock, is constituted of fine-grained clay particles that have undergone compaction. It forms as a result of clay deposition in tranquil aquatic environments, such as lakes, lagoons, or deep-sea settings.

The concentrations of Na_2O, MgO, Al_2O_3, SiO_2, K_2O, CaO, TiO_2, and Fe-oxides within sedimentary rocks typically surpass 0.1%, and are classified as major elements. These major elements constitute a critical component of inorganic minerals present in sedimentary rocks and serve as significant determinants influencing the industrial characteristics and processing applications of coal (Seredin and Dai, 2012; Finkelman *et al.*, 2019; Dai *et al.*, 2020). Despite the contributions of prior scholars who have investigated the geochemical characteristics of the mudstones originating from the Gombe formation (Mohammed *et al.*, 2018; Ayinla *et al.*, 2017a, 2017b; Usman *et al.*, 2017), a comprehensive analysis of major oxides geochemistry remains absent or poorly documented. Therefore, there exists a necessity for an extensive examination of major oxides geochemistry pertaining to the mudstones of the Gombe formation. To fulfill this objective, a total of twenty outcrop samples were systematically collected through sedimentological methods, subsequently analyzed using x-ray fluorescence spectrometry (XRF), resulting in the identification and examination of twenty major oxides.

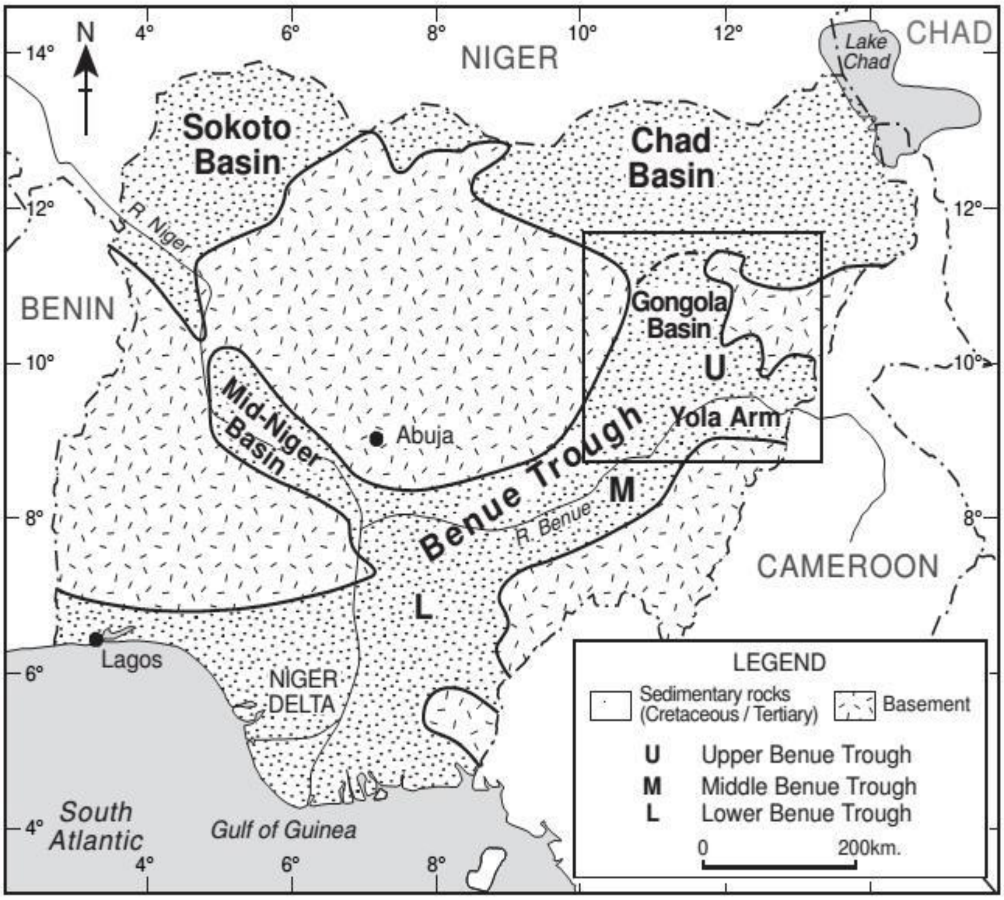

Fig. 1: Generalised geological map of Nigeria showing the location of the Gongola Basin (Abubakar, 2014).

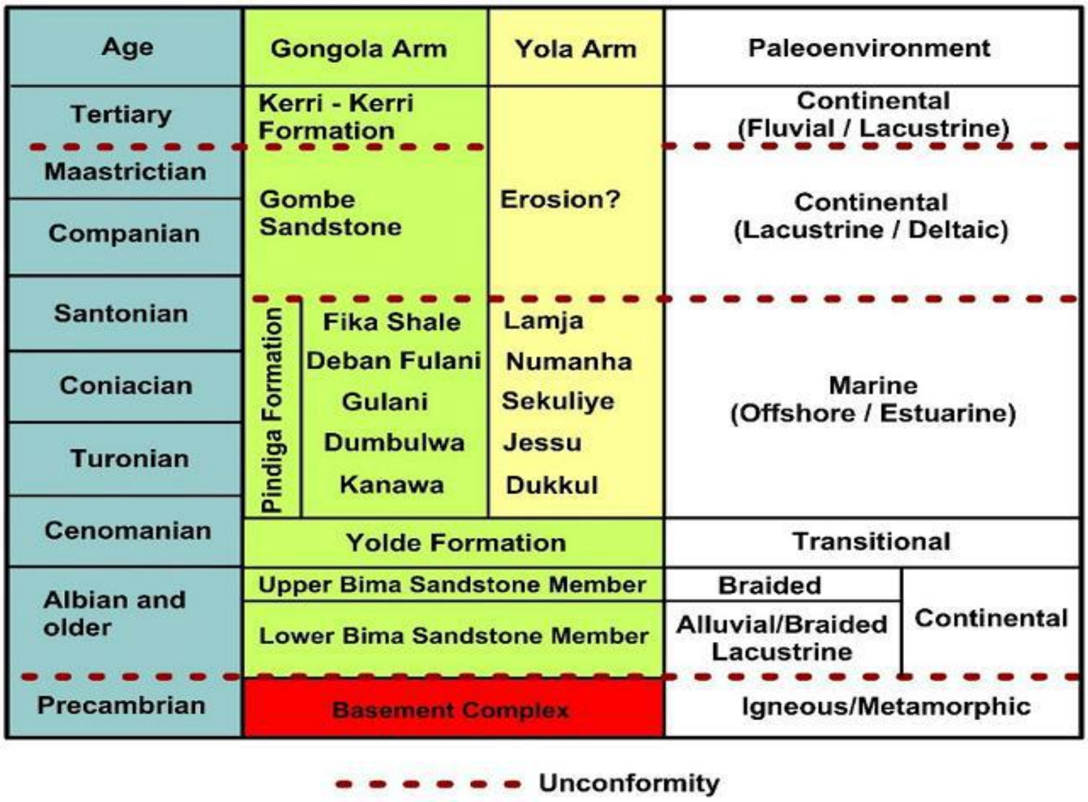

Fig. 2: Stratigraphic successions of Upper Benue Trough (Obaje *et al.*, 2006)

METHODOLOGY

Sampling

The difficulties associated with acquiring subsurface samples, in light of governmental regulations, necessitated the employment of outcrop samples in this investigation. In total, 20 outcrop samples were collected from shaly mudstone sequences within the Gombe Formation located in the Gongola Basin (Fig. 3), which embody various sedimentary logs and facies. Given that weathering consistently poses a significant concern for inorganic geochemical analyses of outcrop sediments, weathered rock surfaces were excised by excavating to an approximate depth of 0.5 m at each sampling location to obtain fresh and unweathered samples.

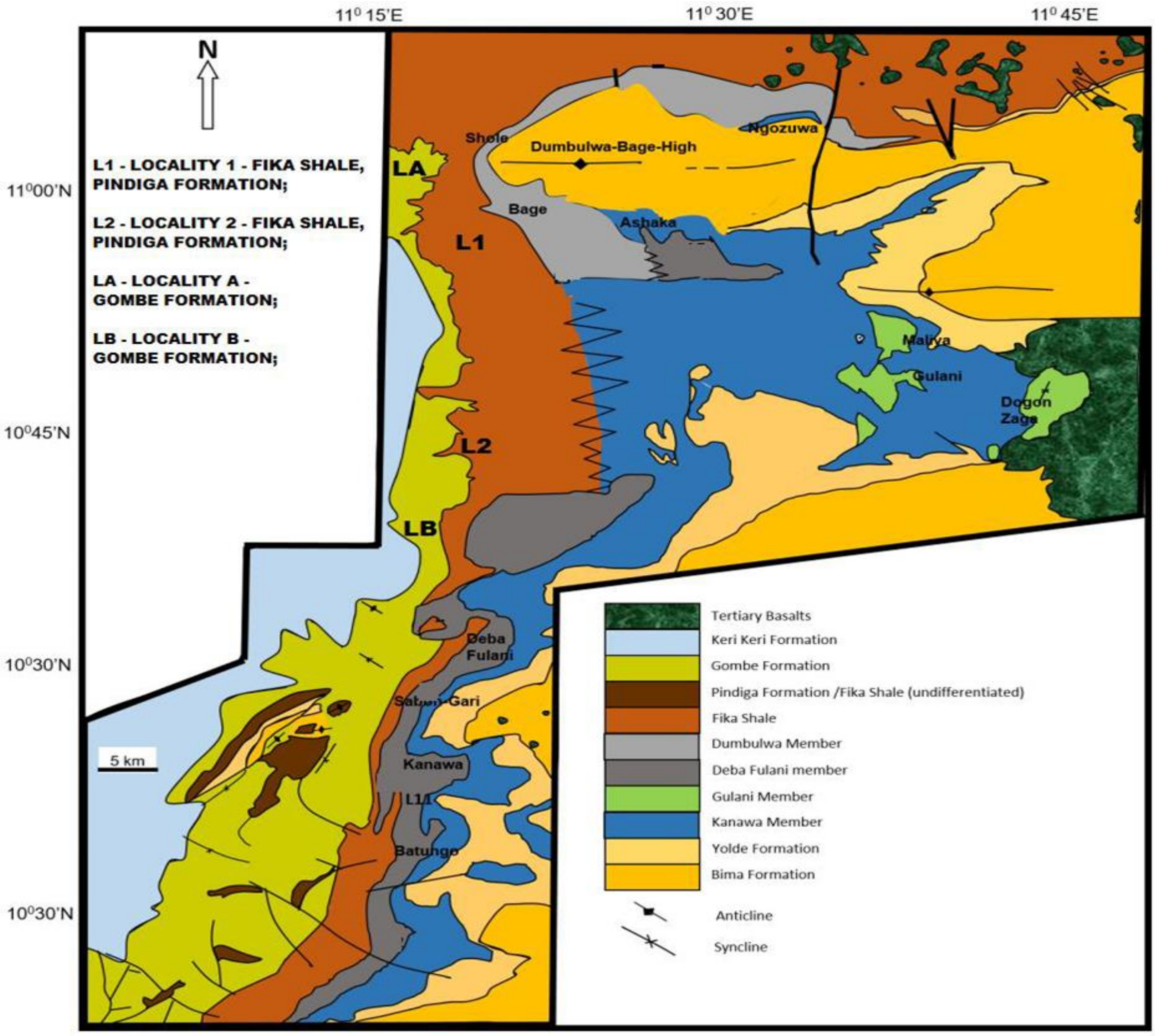

Fig. 3: Geological map of Gongola Basin showing the study areas and sampling (modified after Goro *et al*., 2021).

Sample preparation

All the glasswares employed in the experimental procedure underwent comprehensive washing and rinsing with distilled water. Thereafter, they were subjected to immersion in a chromic acid solution for a duration of 24 hours. Subsequently, the glasswares were meticulously rinsed utilizing deionized distilled water, followed by a drying in an oven maintained at a temperature of 110˚C. Then, they were transferred to desiccators for cooling purposes (Akinlua *et al*., 2008). The mudstone samples were processed via grinding utilizing an agate mortar. The resulting pulverized samples were individually sifted through a sieve with a mesh size of 100um. To prevent cross-contamination, the pestle and mortar were scrupulously cleaned after the grinding of each sample.

X-ray fluorescence spectrometry (XRF) analysis
4g rock powders with a grain size of approximately 300 meshes underwent compression to form a pellet inside a disk measuring 32mm in diameter at a pressure of 32MPa. Subsequently, the pellets were analyzed at the analytical laboratory, Department of Chemistry, Umaru Musa University, Katsina State, Nigeria using an Axios 4.0 X-ray fluorescence spectrometer. The operational parameters for the XRF machine included V=60kV, I=120mA, and P=4kW. To ensure the accuracy of major oxide measurements, the average precision was maintained at below 2%. The results of major oxides are presented in Table 1.

RESULTS AND DISCUSSION

Distribution of Major Oxides
The concentrations of the major oxides in the mudstones obtained from the Gombe Formation are presented in Table 1. A total of twenty (20) major oxides were identified in the mudstones, which includes SiO_2, Al_2O_3, Fe_2O_3, TiO_2, MgO, K_2O, P_2O_5, SO_3, ZrO_2, SrO, MnO, CaO, and Cl (Table 1). The mean concentrations of the major oxides exhibit a range from 0.01 to 38.09 % (Table 1, Fig. 4). SiO_2 demonstrates the highest concentration, recording the mean value of 38.09 %. SiO_2 is primarily sourced from the remnants of ancient marine organisms that inhabited the oceanic environments during the deposition of the mudstones (Niu et al., 2015). This is subsequently followed by Al_2O_3, Fe_2O_3, MgO, TiO_2, K_2O, BaO, and SrO, which have the mean values of 15.67 %, 3.36 %, 2.48 %, 2.19 %, 1.00 %, and 0.65 %, respectively (Table 1, Fig. 6), while the concentrations of the remaining oxides are low (Table 1, Fig. 4).

Table 1: Concentrations of the major oxides in the studied mudstones

Samples	Fe_2O_3 (%)	SiO_2 (%)	Al_2O_3 (%)	MgO (%)	P_2O_5 (%)	SO_3 (%)	TiO_2 (%)	MnO (%)	CaO (%)
SGF-1	2.86	37.46	19.5	2.58	0.01	0.14	0.45	0.1	0.23
SGF-2	2.27	40.93	17.51	2.36	0.02	0.33	1.44	0.1	0.25
SGF-3	1.97	42.94	18.88	1.69	0.02	0.22	1.51	0.09	0.22
SGF-4	2.34	37.17	18.75	1.62	0	0.33	1.48	0.08	0.24
SGF-5	2.37	37.81	19.19	1.8	0.01	0.16	1.48	0.09	0.26
SGF-6	1.64	42.66	17.64	2.98	0.07	0.52	1.39	0.09	0.23
SGF-7	2.24	39.41	21.94	4.51	0.1	0.28	1.51	0.1	0.23
SGF-8	2.13	36.22	20.59	2.1	0	0.29	1.38	0.09	0.23
SGF-9	1.53	41.84	17.47	3.73	0.06	0.52	1.24	0.07	0.2
SGF-10	1.33	43.86	17.95	2.69	0.07	0.69	1.37	0.08	0.22
SGF-11	1.81	42.28	16.23	2.75	0	0.27	1.41	0.09	0.3
SGF-12	6.89	30.6	12.01	2.39	0.01	0.11	0.95	0.56	0.47
SGF-13	6.42	37.4	11.61	2.46	0	0.06	0.84	0.52	0.29
SGF-14	5.41	39.88	10.5	2.85	0	0.07	1.04	0.49	0.24
SGF-15	9.58	4.17	1.84	0.97	0.61	0.04	21.53	0.89	0.13
SGF-16	3.03	49.64	9.65	2.29	0	0.05	0.31	0.27	0.28
SGF-17	4	49.4	8.43	2.8	0	0.06	0.77	0.14	0.3
SGF-18	2.19	37.17	20.56	2.68	0.01	0.13	1.43	0.1	0.23
SGF-19	2.04	36.22	20.5	1.82	0	0.19	1.49	0.09	0.24
SGF-20	5.18	34.78	12.64	2.45	0.11	0.36	0.78	0.19	1.17
Mean	3.36	38.09	15.67	2.48	0.06	0.24	2.19	0.21	0.30

Table 1: Contd

Samples	K_2O (%)	CuO (%)	ZnO (%)	Cr_2O_3 (%)	V_2O_5 (%)	PbO (%)	Cl (%)	ZrO_2 (%)	SrO (%)	BaO (%)	SnO_2 (%)	LOI
SGF-1	0.98	0.01	0.02	0.01	0.05	0.01	0.03	0.02	0.38	1	0.27	33.89
SGF-2	1.26	0.01	0.02	0.01	0.05	0.01	0.03	0.05	0.49	1	0	31.86
SGF-3	1.2	0.01	0.02	0.01	0.05	0.01	0.02	0.04	0.46	1	0	29.64
SGF-4	1.01	0.01	0.02	0.01	0.05	0.01	0.01	0.03	0.59	1	0	35.25
SGF-5	0.99	0.01	0.02	0.01	0.05	0.01	0.01	0.03	0.53	1	0	34.17
SGF-6	1.21	0.01	0.01	0.01	0.04	0.01	0.01	0.04	1.5	1	0	28.94
SGF-7	1	0.01	0.02	0.01	0.04	0.01	0.01	0.06	0.94	1	0	26.58
SGF-8	0.86	0.01	0.02	0.01	0.05	0.01	0.02	0.03	0.46	1	0	34.5
SGF-9	1.06	0.01	0.01	0	0.04	0.01	0.01	0.04	1.12	1	0	30.04
SGF-10	1.25	0.01	0.01	0.01	0.04	0.01	0.02	0.04	1.19	1	0	28.16
SGF-11	1.19	0.01	0.01	0.01	0.04	0	0.03	0.5	0.4	1	0.3	31.37
SGF-12	2.13	0.06	0.03	0.01	0.05	0	0.01	0.01	0.25	1	0	42.46
SGF-13	2.11	0.03	0.02	0.01	0.04	0	0.01	0.01	0.24	1	0	36.93
SGF-14	1.98	0.02	0.02	0.01	0.04	0.01	0.01	0.01	0.23	1	0	36.19
SGF-15	0.06	0.01	0.01	0	0.6	0.01	0	0.65	0.22	1	0	57.68
SGF-16	0.77	0.02	0.01	0.01	0.02	0.01	0.01	0.02	0.29	1	0	32.32
SGF-17	1.08	0.02	0.01	0.01	0.03	0.01	0.01	0.02	0.23	1	0.23	31.45
SGF-18	0.88	0.01	0.02	0.01	0.06	0.01	0.01	0.02	0.47	1	0	33.01
SGF-19	0.88	0.02	0.02	0.01	0.06	0.01	0.01	0.01	0.4	1	0	34.99
SGF-20	1.19	0.01	0.02	0.01	0.05	0.01	0.01	0	2.67	1	0	37.37
Mean	1.15	0.02	0.02	0.01	0.07	0.01	0.01	0.08	0.65	1	0.04	34.34

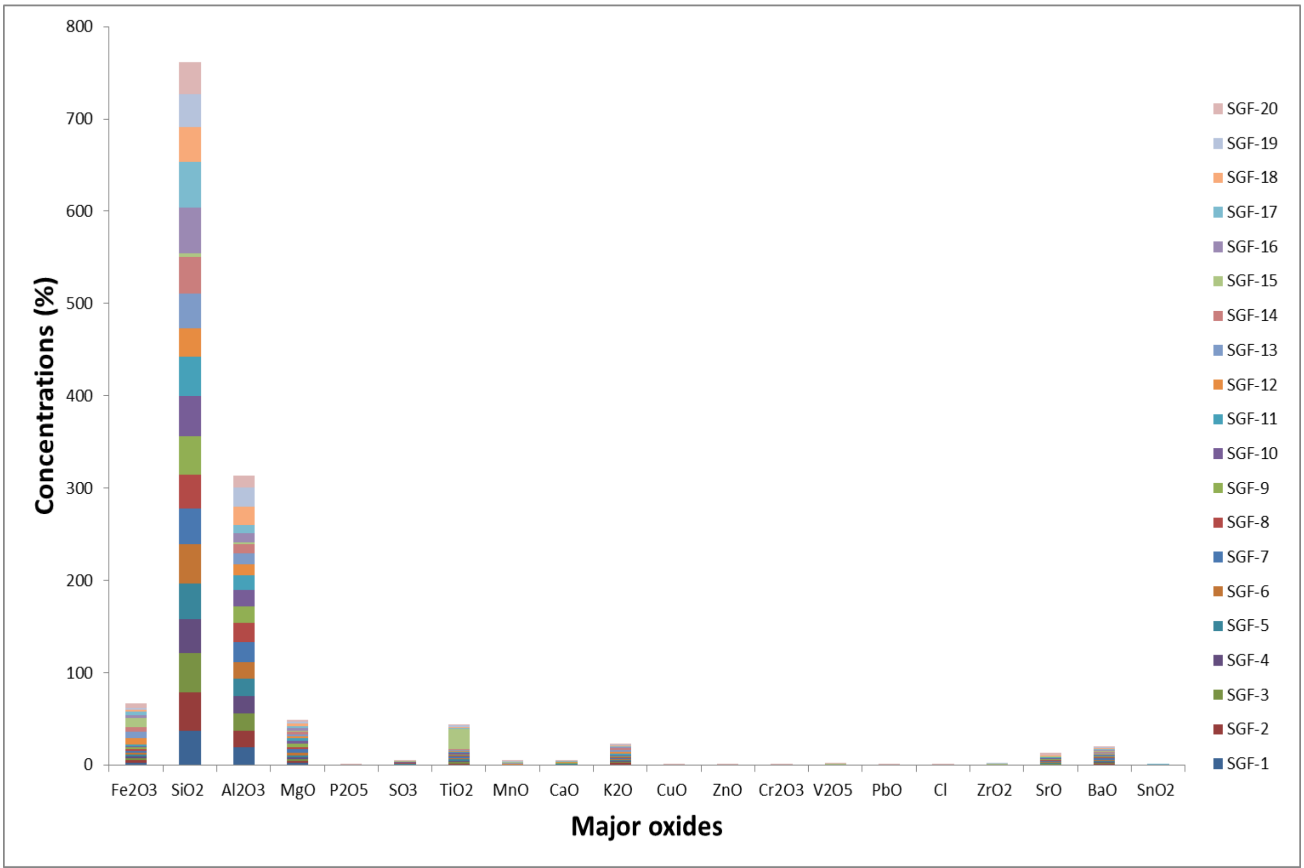

Fig. 4.: The histogram of the contents of the major oxides in the studied mudstones.

As reported by Yang and Du (2017), Al_2O_3 and Fe_2O_3 originate from the weathering processes of aluminum- and iron-rich minerals that were present in the source area of the mudstones. Moreover, the detection of calcium oxide (CaO; with the mean value of 0.30 %) and magnesium oxide (MgO; with the mean value of 2.48 %) within the mudstones in relatively substantial quantities implies contributions from marine environments and the weathering of calcium- and magnesium-rich minerals in the parent rock (Niu *et al.*, 2015). This distribution pattern has been documented in earlier studies of Eocene to Recent sediments from the Western Niger Delta, Nigeria (Edema *et al.*, 2016). Furthermore, Pundaree *et al.* (2015) observed that mafic rocks are predominantly characterized by Fe_2O_3 and MgO. Consequently, the comparatively elevated concentrations of Fe_2O_3 (with the mean value of 3.36%) and MgO (with the mean value of 2.48 %) in the analyzed samples suggest that the source rocks are likely to be classified as mafic to ultramafic in nature. The absence of sodium oxide (Na_2O) from the Gombe mudstones indicates that the mudstones may have been deposited in a reducing environment. Under reducing conditions, sodium cations may be extracted from the sediment via interactions with organic matter or sulfide compounds. Furthermore, in instances where the sedimentary basin is situated at a considerable distance from the origin of sodium-rich minerals, the availability of sodium may be insufficient for the synthesis of Na_2O. The substantial concentration of SiO_2 observed in the Gombe mudstone samples, which varied from 4.17% to 49.64% with the mean value of 38.09% (Table 1), implies that these mudstones are predominantly quartz-rich sedimentary rocks, such as sandstone, which exhibits remarkable resistance to weathering attributable to its elevated quartz composition (Nesbitt and Young, 1982). Nevertheless, the presence of Fe_2O_3, which ranges between 1.64% and 9.58% with the mean value of 3.36%, alongside Al_2O_3, ranging from 1.84% to 21.94% with the mean value of 15.67% (Table 1), in both considerable quantities, signifies that the rock has experienced a certain level of weathering, as these oxides are conventionally linked to the degradation of iron-rich minerals and feldspars, respectively (Federman *et al.*, 1999).

The Al_2O_3 plots against selected major oxides as plotted in Figures 5 and 6 show weak positive correlations against SiO_2 and MgO, and negative correlations against other oxides, which probably imply that these major oxides are not only hosted by clay minerals (Li *et al.*, 2019). Except for SiO_2 and MgO, the other oxides weakly follow the trend of negative correlation (increasing as Al_2O_3 increases), indicating that quartz content is not influenced by a special paleoenvironment favoring the growth of siliceous tests and skeletons (e.g. radiolarian or siliceous sponges) (Li *et al.*, 2019). Also, K_2O and MgO show positive correlations on the plots of SiO_2 versus major elements (figures 7 and 8) while others are negative which further suggests that they are associated with micaceous and/or clay minerals in the sediments (Pundaree *et al.*, 2015). A negative relationship between CaO and MgO is detected, suggesting that these mudstones are composed of minerals other than carbonates (Fig. 8d). Considering the lower LOI which is mainly attributed to losses of CO_2 and organic matters (Table 1), enrichment of CaO and MgO in these shales is possibly resulted from carbonate minerals.

Provenance

The discrimination diagram proposed by Roser and Korsch (1986) for the classification of sedimentary origins into four distinct provenance zones—namely, mafic, intermediate, felsic, and igneous provenances—was deemed inapplicable in the context of the current investigation, due to the absence of Na_2O among the primary oxides. The ratios of Al_2O_3/TiO_2 in rocks and sediments serve primarily to deduce the compositional characteristics of the source rocks. Hayashi *et al.* (1997) demonstrated that Al_2O_3/TiO_2 ratios ranging from 21 to 70, 8 to 21, and 3 to 8 correspond to felsic igneous, intermediate, and mafic igneous rocks, respectively. The values recorded (0.09 to 43.33%, with the mean value of 14.88, as shown in

Table 2) in the analyzed mudstones imply that the sediments originated from a mixture of felsic igneous to mafic igneous rock types. Furthermore, the SiO_2/Al_2O_3 ratio values were employed to assess the compositional maturity of these sediments. It is widely recognized that this particular ratio exhibits elevated values when the sediment composition is considered mature. Roser *et al.* (1996) established that basic igneous rocks possess a SiO_2/Al_2O_3 value of 3, while acidic igneous rocks typically exhibit a ratio of approximately 5. Consequently, values exceeding 5 in clastic deposits are indicative of sedimentary maturity. The SiO_2/Al_2O_3 values of the mudstones examined in this study range between 1.77 and 5.86, with the mean value of 2.43 (Table 2), thereby suggesting a mixed compositional maturity (Table 2). The cross plots of TiO_2 and K_2O relative to Al_2O_3, illustrated in Figure 9, indicate that the mudstones are primarily comprised of basalt, granite, and muscovite minerals (Hayashi *et al*., 1997).

Tectonic settings

The comprehension of the tectonic settings of a basin is paramount in the exploration of petroleum and other economically significant resources, as well as in the discipline of paleogeography. A multitude of scholars has underscored the importance of utilizing major element geochemical analysis of sedimentary rocks to infer tectonic environments through the application of discrimination diagrams (for instance, Roser and Korsch, 1986; Bhatia, 1983). Nevertheless, the application of these diagrams was precluded in the present investigation due to the lack of Na_2O among the major oxides. Consequently, we employed the diagrams of Fe_2O_3+MgO versus TiO_2 and Al_2O_3/SiO_2 (Bhatia, 1983) (Fig. 10). These discrimination diagrams proficiently categorize the tectonic settings into four discrete zones: oceanic island arc, continental island arc, active continental margin, and passive margin. In the current study, the mudstones were grouped in proximity to the active continental margin on the plots of Fe_2O_3+MgO versus TiO_2 (Fig. 10a) and Fe_2O_3+MgO versus Al_2O_3/SiO_2 (Fig. 10b).

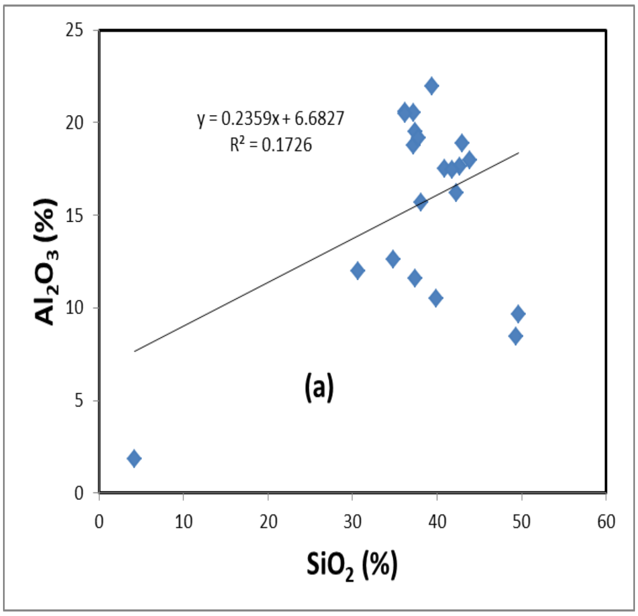

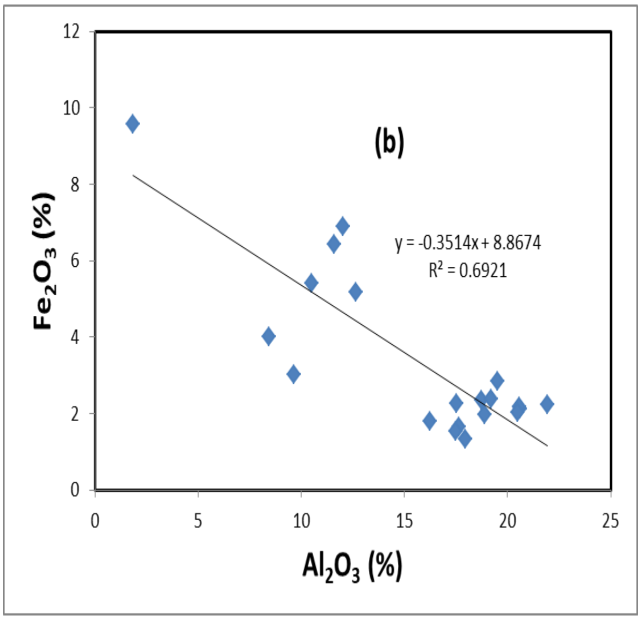

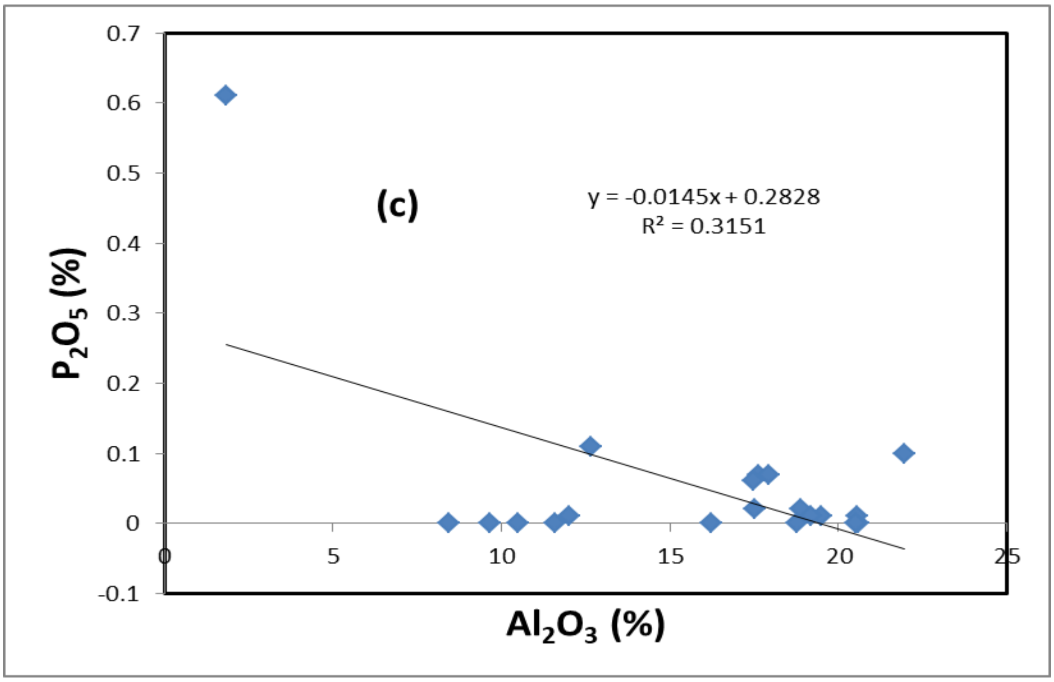

Fig. 5: Correlation plots of Al_2O_3 vs (a) SiO_2, (b) Fe_2O_3, and (c) P_2O_5 in Gombe mudstones.

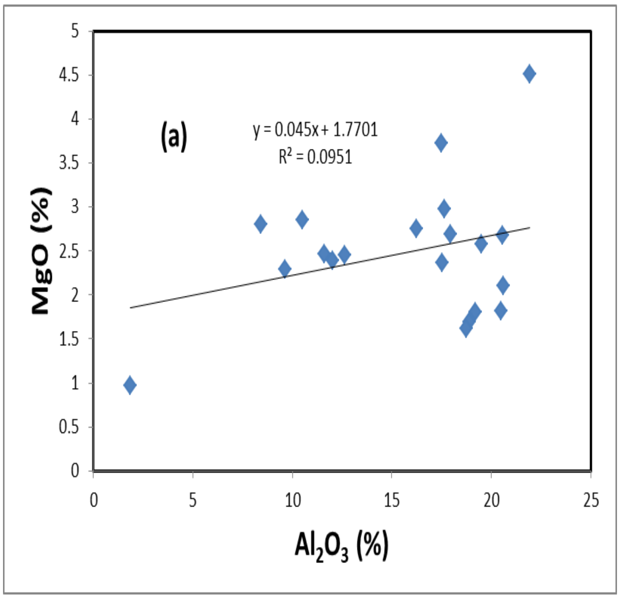

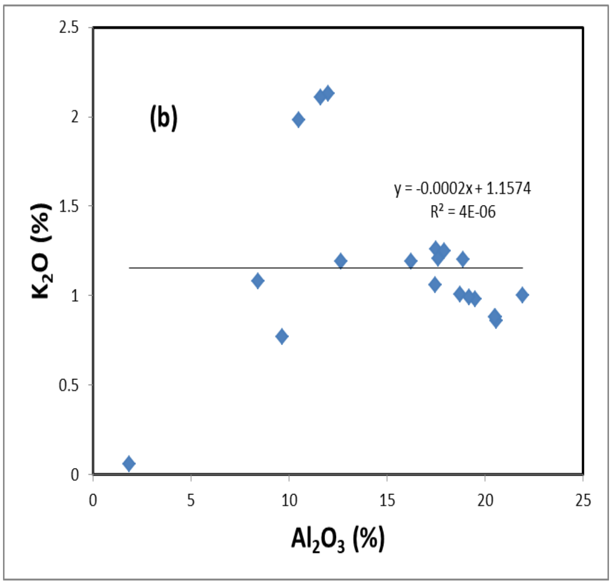

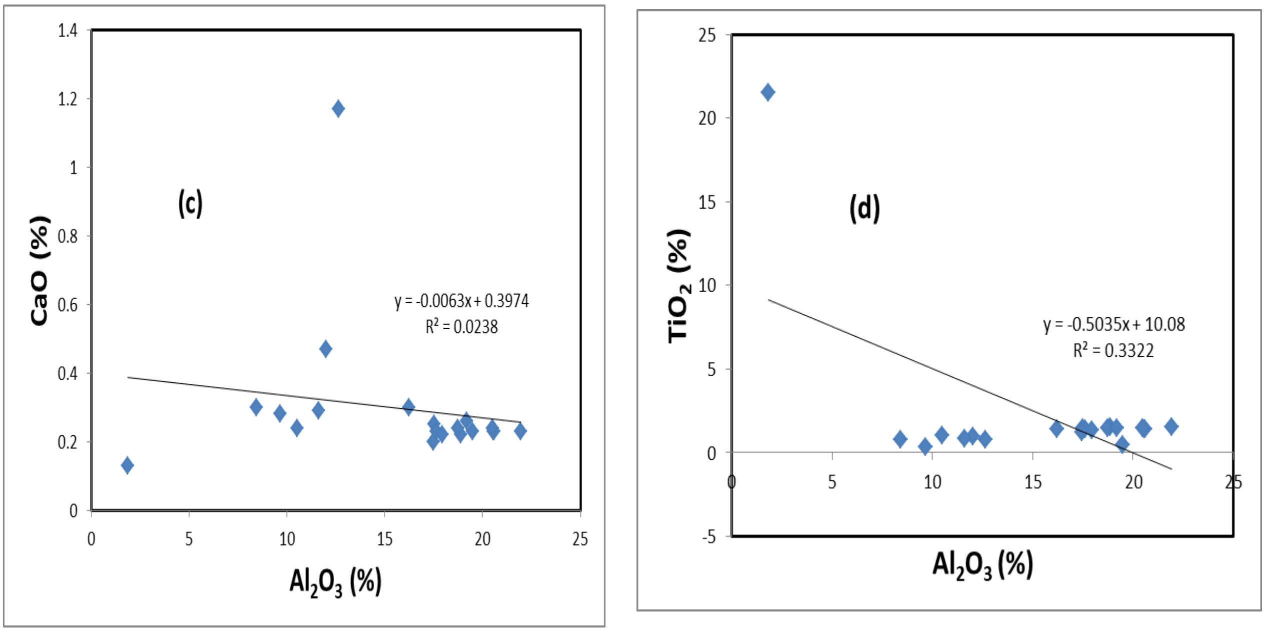

Fig. 6: Correlation plots of Al_2O_3 vs (a) MgO, (b) K_2O, (c) CaO, and (d) TiO_2 in Gombe mudstones.

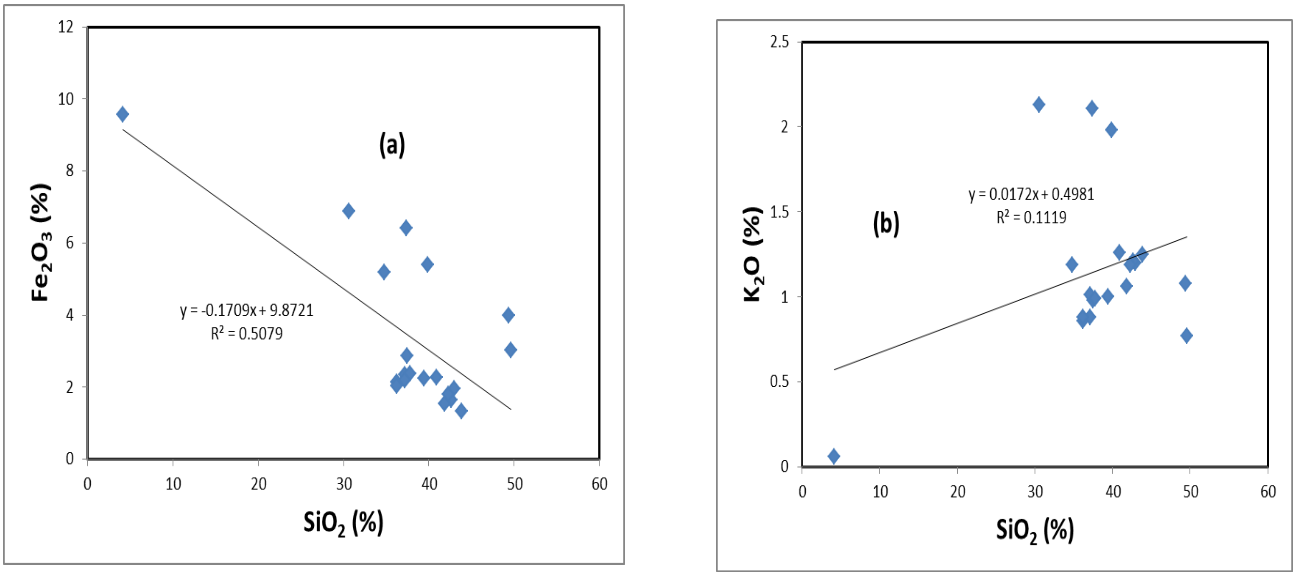

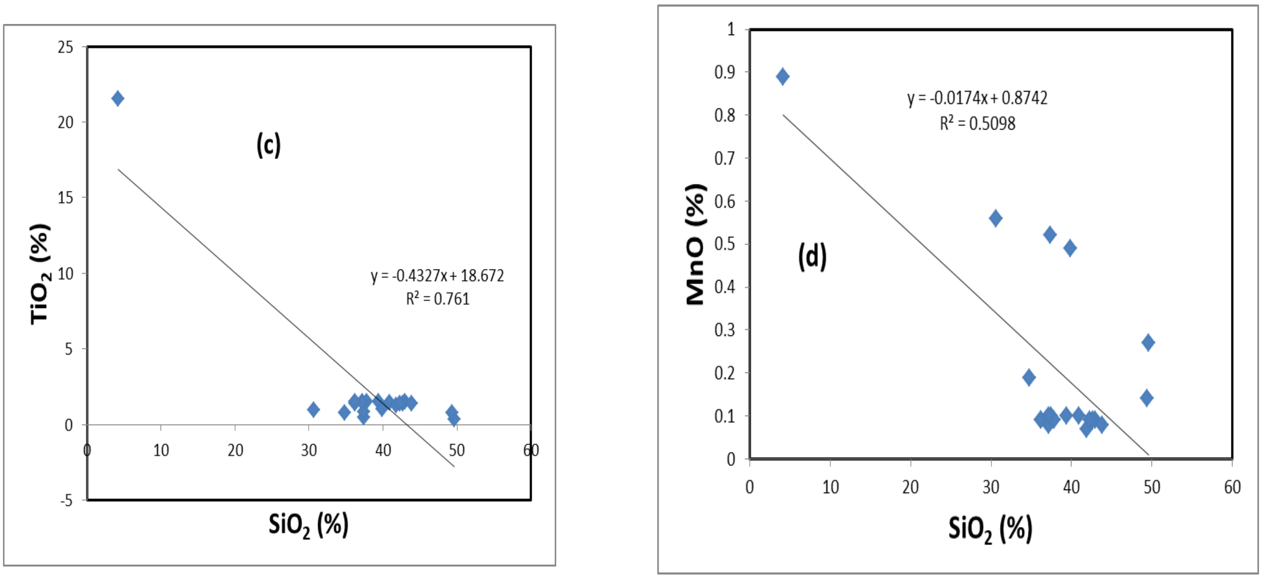

Fig. 7: Correlation plots of SiO_2 vs (a) Fe_2O_3, (b) K_2O, (c) TiO_2, and (d) MnO in Gombe mudstones.

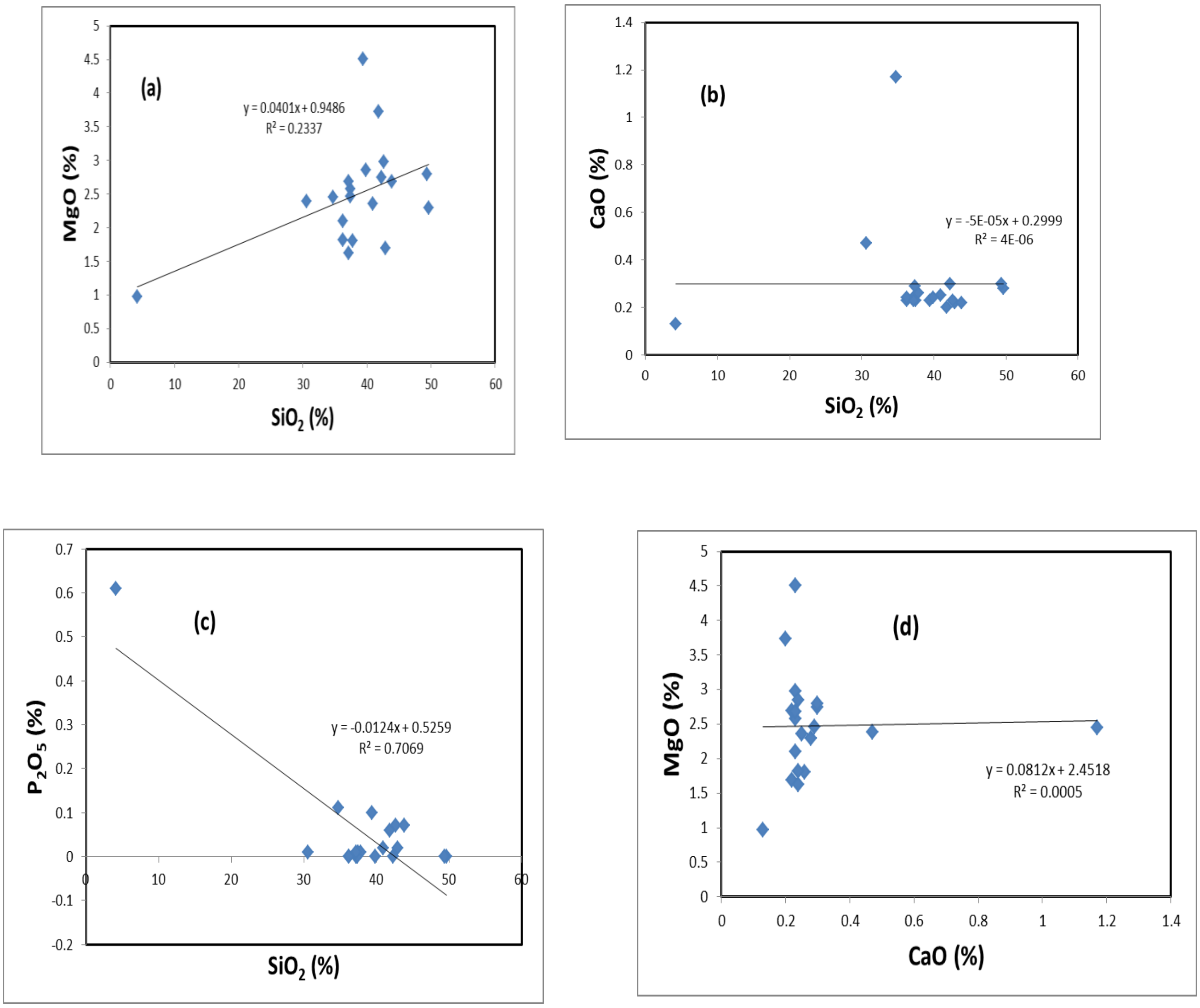

Fig. 8: Correlation plots of SiO_2 vs (a) MgO, (b) CaO, (c) P_2O_5, and (d) Plot of MgO vs. CaO in Gombe mudstones.

Table 2: Geochemical ratios computed from the major oxides in the mudstones

Samples	Al_2O_3/TiO_2	MgO/Al_2O_3	K_2O/Al_2O_3	CaO/Al_2O_3	Fe_2O_3/Al_2O_3	SiO_2/Al_2O_3	SiO_2/TiO_2	Fe_2O_3/K_2O
SGF-1	43.33	0.13	0.05	0.01	0.15	1.92	83.24	2.92
SGF-2	12.16	0.13	0.07	0.01	0.13	2.34	28.42	1.80
SGF-3	12.50	0.09	0.06	0.01	0.10	2.27	28.44	1.64
SGF-4	12.67	0.09	0.05	0.01	0.12	1.98	25.11	2.32
SGF-5	12.97	0.09	0.05	0.01	0.12	1.97	25.55	2.39
SGF-6	12.69	0.17	0.07	0.01	0.09	2.42	30.69	1.36
SGF-7	14.53	0.21	0.05	0.01	0.10	1.80	26.10	2.24
SGF-8	14.92	0.10	0.04	0.01	0.10	1.76	26.25	2.48
SGF-9	14.09	0.21	0.06	0.01	0.09	2.39	33.74	1.44
SGF-10	13.10	0.15	0.07	0.01	0.07	2.44	32.01	1.06
SGF-11	11.51	0.17	0.07	0.02	0.11	2.61	29.99	1.52
SGF-12	12.64	0.20	0.18	0.04	0.57	2.55	32.21	3.23
SGF-13	13.82	0.21	0.18	0.02	0.55	3.22	44.52	3.04
SGF-14	10.10	0.27	0.19	0.02	0.52	3.80	38.35	2.73
SGF-15	0.09	0.53	0.03	0.07	5.21	2.27	0.19	159.67
SGF-16	31.13	0.24	0.08	0.03	0.31	5.14	160.13	3.94
SGF-17	10.95	0.33	0.13	0.04	0.47	5.86	64.16	3.70
SGF-18	14.38	0.13	0.04	0.01	0.11	1.81	25.99	2.49
SGF-19	13.76	0.09	0.04	0.01	0.10	1.77	24.31	2.32
SGF-20	16.21	0.19	0.09	0.09	0.41	2.75	44.59	4.35
Average	14.88	0.19	0.08	0.02	0.47	2.43	17.39	2.91

Paleosalinity and detrital influx

Typically, elevated levels of P_2O_5 are commonly found in dysaerobic water close to the transition between oxic and anoxic conditions; therefore, fluvial swamps exhibit relatively low (0.01%) P_2O_5 (Demaison and Moore, 1980). The P_2O_5 concentrations range from 0.01 wt% to 0.61 wt% in the analyzed mudstones, indicating the influence of fluvial processes (Table 1). The increased P_2O_5 levels identified in SGF-15 could be attributed to the influx of detrital material with high mineral contents (Akinyemi *et al*., 2022).

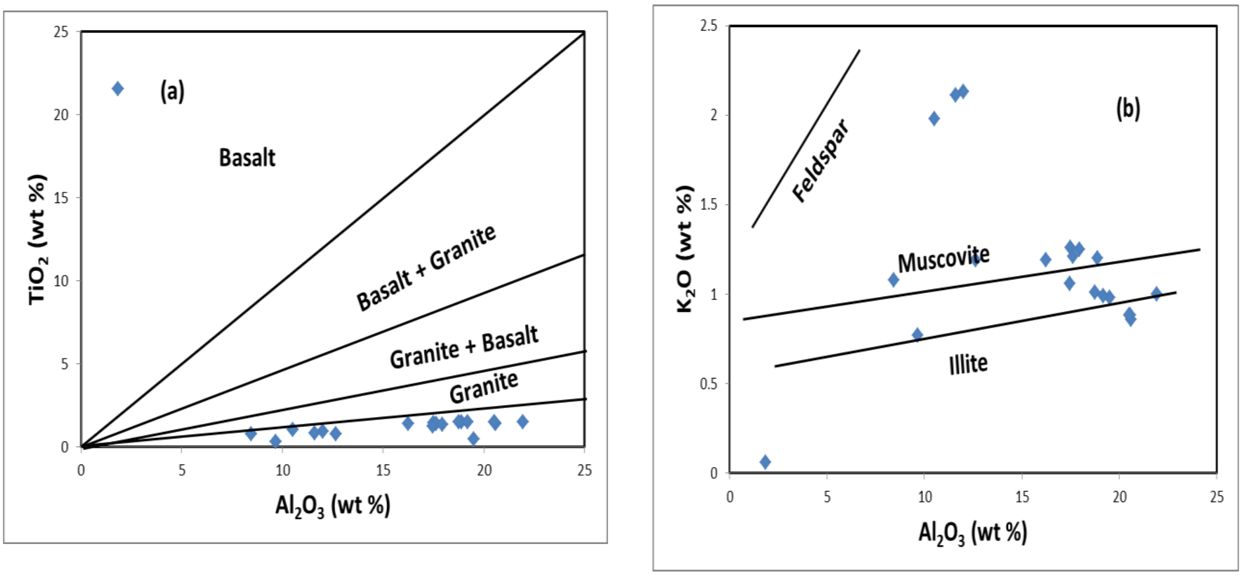

Fig. 9: Cross plots of Al_2O_3 vs (a) TiO_2 (after Hayashi et al., 1997) and (b) K_2O (after Hayashi *et al*., 1997).

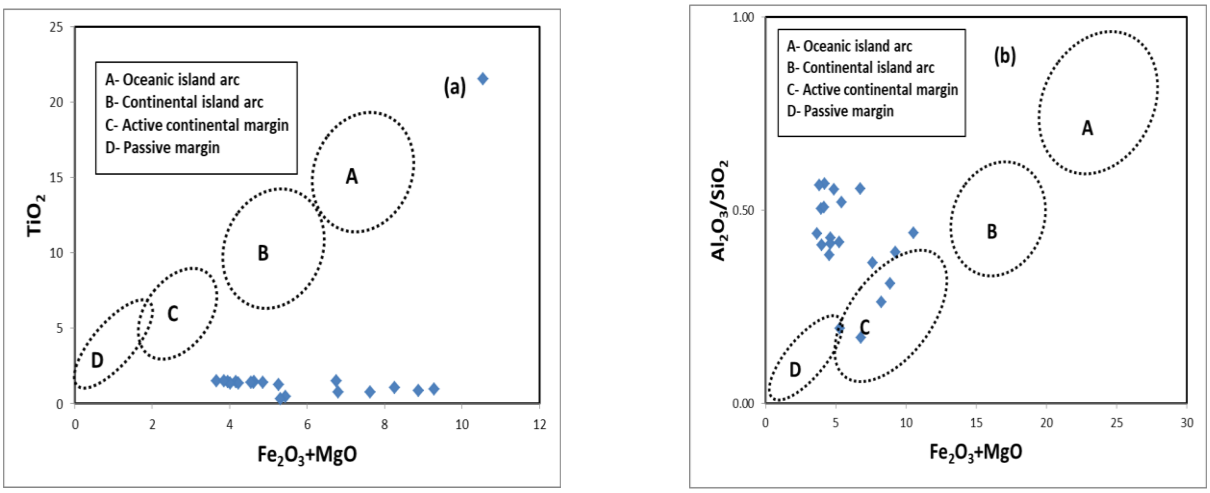

Fig. 10: Cross plots of Fe_2O_3 + MgO vs. (a) TiO_2 (after Bhatia., 1983) and (b) Al_2O_3/SiO_2 (after Bhatia, 1983) in the studied mudstones.

CONCLUSION

Among the major oxides detected, SiO_2 has the highest concentration, followed by Al_2O_3>Fe_2O_3 > MgO>TiO_2>K_2O>BAO>SrO while most others had low values, implying mudstones composed principally of quartz minerals and deposited in marine environments. The low P_2O_5 concentrations recorded in the analyzed mudstones indicated the influence of fluvial processes. Additionally, the geochemical ratios computed from the major oxide in the mudstones indicated that the sediments were derived from a mixture of felsic igneous to mafic igneous rocks and mixed compositional maturity near the active continental margin. The investigation demonstrated that the geochemical analysis of major oxides proved to be a valuable method for assessing the provenance, tectonic conditions, and palaeosalinity of mudstone deposits.

REFERENCES

Abubakar, M.B. (2014). Petroleum Potentials of the Nigerian Benue Trough and Anambra Basin: A Regional Synthesis. *Natural Resources* 5(1): 25–58.

Akinlua, A., Torto, N. and Ajayi, T.R. (2008). Determination of rare earth elements in Niger Delta crude oils by inductively coupled plasma-mass spectrometry. *Fuel* 87: 1469-1477.

Akinyemi, S.A., Adebayo, O.F., Madukwe, H.Y., Kayode, A.T., Aturamu, A.O., OlaOlorun, O.A., Nyakuma, B.B, Jauro, A., Gitari, W.M., Mudzielwana, R. and Hower, J.C. (2022). Elemental geochemistry and organic facies of selected Cretaceous coals from the Benue Trough basin in Nigeria: Implication for paleodepositional environments. *Marine and Petroleum Geology* 137: 105490.

Ayinla, H.A., Abdullah, W.H., Makeen, Y.M., Abubakar, M.B., Jauro, A., Sarki Yandoka, B.M., Mustapha, K.A. and Abidin, N.S.Z. (2017a). Source rock characteristics, depositional setting and hydrocarbon generation potential of Cretaceous coals and organic rich mudstones from Gombe Formation, Gongola Sub-basin, Northern Benue Trough, NE Nigeria. *International Journal of Coal Geology* 173:212–226.

Ayinla, H.A., Abdullah, W.H., Makeen, Y.M., Abubakar, M.B., Jauro, A., Sarki Yandoka, B.M., Mustapha, K.A. and Abidin, N.S.Z. (2017b). Petrographic and geochemical characterization of the Upper Cretaceous coal and mudstones of Gombe Formation, Gongola sub-basin, northern Benue trough Nigeria: Implication for organic matter preservation, paleodepositional environment and tectonic settings. *International Journal of Coal Geology* 180: 67–82.

Bhatia, M.R. (1983). Plate tectonics and geochemical composition of sandstones: *Journal of Geology* 91: 611-627.

Benkhelil, J. (1989). The origin and evolution of the cretaceous Benue Trough (Nigeria). J. *Afr. Earth Sci*. 8 (2–4): 251–282.

Dai, S., Hower, J.C., Finkelman, R.B., Graham, I.T., French, D., Ward, C.R., Eskenazy, G., Wei, Q. and Zhao, L. (2020). Organic associations of non-mineral elements in coal: A review. *Int. J. Coal Geol*. 218: 103347. https://doi.org/10.1016/j. coal.2019.103347.

Demaison, G.J. and Moore, G.T. (1980). Anoxic environments and oil source bed genesis. *AAPG (Am. Assoc. Pet. Geol.) Bull.* 64 (8): 1179–1209.

Edema, A.A., Olatunji A.S. and Bamidele, O. (2016). Inorganic Geochemical Evaluation and Aspects of Rock Eval Pyrolysis of Eocene to Recent Sediments of Soso and Kay-1 Wells, Western Niger Delta, Nigeria. *Journal of Environment and Earth Science* 6 (10): 67-90.

Fatoye, F.B. and Gideon, Y.B. (2013a). Appraisal of the economic geology of Nigerian coal resources. *J. Environ. Earth Sci.* 3 (11): 25–31.

Federman, A.N., Grotzinger, J.P. and Milliken, R.E. (1999). Mineralogy and sedimentology of a sulfate-rich outcrop of the Burns Formation (MER) on the plains of Gusev crater, Mars. *Journal of Geophysical Research: Planets* 104(E4): 8673-8715.

Finkelman, R.B., Dai, S. and French, D. (2019). The importance of minerals in coal as the hosts of chemical elements: A review. *Int. J. Coal Geol*. 212: 103251. https://doi. org/10.1016/j.coal.2019.103251.

Goro, I.S., Abubakar, M.B., Bukar, S. and Abdullah, W.H. (2021). Sedimentology and stratigraphy development of sandy members of Pindiga formation, Gongola sub-basin, northern Benue trough, Nigeria: A mixed wave, tide and fluvially…. *Journal of African Earth Sciences* 173: 104024.

Hayashi, K.I., Fujisawa, H., Holland, H.D. and Ohmoto, H. (1997). Geochemistry of ~1.9 Ga sedimentary rocks from northeastern Labrador, Canada. *Geochem. Cosmochim. Acta* 61: 4115–4137.

Idowu, J. and Ekweozor, C. (1993). Petroleum potential of cretaceous shales in the upper Benue Trough, Nigeria. *J. Petrol. Geol*. 16 (3): 249–264.

Li, H., Liu, B., Liu, X., Meng, L., Cheng, L. and Wang, H. (2019). Mineralogy and inorganic geochemistry of the Es4shales of the Damintun Sag, northeast of the Bohai Bay basin: Implication for depositional environment. *Marine and Petroleum Geology* 110: 886–900.

Mohammed, YB., Hamza, H. and Shettima, B. (2018). Geochemical Assessment of Mudstone Member of the Gombe (Sandstone) Formation, Gombe and Environs, Gongola Basin. *IOSR Journal of Applied Geology and Geophysics (IOSR-JAGG) 6 (3):21-26.*

Nesbitt, H.W. and Young, G.M. (1982). Early Proterozoic climates and plate motions inferred from major element chemistry of lutites. *Nature* 299: 715–717.

Niu, Y.L., Liu, Y., Xue, Q.Q., Shao, F.L., Chen, S., Duan, M., Guo, P.Y., Gong, H.M., Hu, Y., Hu, Z.X., Kong, J.J., Li, J.Y., Liu, J.J., Sun, P., Sun, W.L., Ye, L., Xiao, Y.Y. and Zhang, Y. (2015). Exotic origin of the Chinese continental shelf: New insights into the tectonic evolution of the western Pacific and eastern China since the Mesozoic. *Science Bulletin* **60**: 1598-1616.

Nwajide, C.S. (2013). Geology of Nigeria's Sedimentary Basins. CSS Bookshops Ltd., Lagos, Nigeria. 565pp.

Nwajide, C. (1990). Cretaceous Sedimentation and Paleogeography of the Central Benue Trough. The Benue. *Tough structure and Evolution International Monograph Series, Braunschweig*, pp. 19–38.

Obaje, N. G., Attah, D.O, Opeloye S.A. and Moumouni A. (2006). Geochemical evaluation of the hydrocarbon prospects of sedimentary basins in Northern Nigeria. *Geochemical Journal* 40: 227 – 243.

Obaje, N., Abaa, S., Najime, T. and Suh, C. (1999). Economic geology of Nigerian coal resources-a brief review. *Afr. Geosci. Rev.* 6: 71–82.

Olade, M. (1975). Evolution of Nigeria's Benue Trough (aulacogen): a tectonic model. *Geol. Mag.* 112 (6): 575–583.

Petters, S.W. (1982). Central west African Cretaceous-Tertiary benthic foraminifera and stratigraphy. *Palaeontograph. Abteilung* 1–104.

Popoff, M., Wiedmann, J. and De Klasz, I. (1986). The Upper Cretaceous Gongila and Pindiga Formations, northern Nigeria: subdivision, age, stratigraphic correlations and paleogeographic implications. *Ecologae Geologicae Helvetiae,* 79: 343-363.

Pundaree, N., Keshav Krishna, A., Subramanyam, K.S.V., Sawant, S.S., Kavitha, S., Kalpana, M.S., Patil, D.J. and Dayal, A.M. (2015). Early Eocene carbonaceous shales of Tadkeshwar Formation, Cambay basin, Gujarat, India: Geochemical implications, petrogenesis and tectonics. *Marine and Petroleum Geology*, http://dx.doi.org/10.1016/j.marpetgeo.2015.08.028

Roser, B.P., Cooper, R.A., Nathan, S. and Tulloch, A.J. (1996). Reconnaissance sandstone geochemistry, provenance, and tectonic setting of the Lower Paleozoic terranes of the West Coast and Nelson, New Zealand. *N. Z. J. Geol. Geophys*. 37 (1): 1–16. https://doi.org/10.1080/00288306.1996.9514690.

Roser, B.P. and Korsch, R.J. (1986). Determination of tectonic setting of sandstone-mudstone suites using SiO_2 content and K_2O/Na_2O ratio. *J. Geol.* 94: 635–650.

Seredin, V.V. and Dai, S. (2012). Coal deposits as potential alternative sources for lanthanides and yttrium. *Int. J. Coal Geol*. 94: 67–93.

Usman, MB, Mamman, YD, Abubakar, U., Sulaiman, A. and Hamidu, H. (2017). Depositional Environment of the Gombe Formation in the Gongola Sub-Basin of the Northern Benue Trough: Using Grain Size Parameters. *Global Journal of Geological Sciences* 15: 25-39.

Yang, J.H. and Du, Y.S. **(**2017**)**. Weathering geochemistry and palaeoclimate implication of the Early Permian mudstones from eastern Henan Province, North China. *Journal of Palaeogeography* 6 (4):370-380.

Zaborski, P. M., Ugodulunwa, F., Idornigie, A., Nnabo, P. and Ibe, K. (1997). Stratigraphy and structure of the Cretaceous Gongola Basin, North-eastern Nigeria. *Bulletin of Centre for Researches Elf Exploration and Production* 21 (1): 153–185.